SAND2017-9739J

Lattice dynamics and thermomechanical properties of zirconium(IV) chloride: Evidence for low-temperature negative thermal expansion

Eunja Kim[a,*], Philippe F. Weck[b], Rosendo Borjas[c], Frederic Poineau[c]

[a]*Department of Physics and Astronomy, University of Nevada Las Vegas, 4505 Maryland Parkway, Las Vegas, NV 89154, USA*
[b]*Sandia National Laboratories, P.O. Box 5800, Albuquerque, NM 87185, USA*
[c]*Department of Chemistry, University of Nevada Las Vegas, 4505 Maryland Parkway, Las Vegas, NV 89154, USA*

Abstract

The crystal structure, lattice dynamics and themomechanical properties of bulk monoclinic zirconium tetrachloride ($ZrCl_4$) have been investigated using zero-damping dispersion-corrected density functional theory [DFT-D3(zero)]. Phonon analysis reveals that $ZrCl_4$(cr) undergoes negative thermal expansion (NTE) near $T \approx 10$ K, with a coefficient of thermal expansion of $\alpha = -1.2$ ppm K^{-1} and a Grüneisen parameter of $\gamma = -1.1$. The bulk modulus is predicted to vary from $K_0 = 8.7$ to 7.0 GPa in the temperature range 0−550 K. The isobaric molar heat capacity derived from phonon calculations within the quasi-harmonic approximation is in fair agreement with existing calorimetric data.

Keywords:

1. Introduction

Zirconium halides are of crucial importance in numerous research fields and industrial applications such as unconvential catalysis (1), refining of Zr-containing ores by Kroll reduction (2), chemical vapor deposition (CVD) (3), or nuclear engineering (4, 5, 6). For example, chlorination has been proposed for large-scale separation and selective recovery of Zr, as $ZrCl_4$, from U−Zr alloys or used nuclear fuel cladding (4, 5). In addition, ZrX_4 (X=Br, Cl) is utilized in the preparation of CVD zirconium carbide layers of tristructural-isotropic (TRISO) nuclear fuel micro-particles (6). Although an accurate knowledge of the properties of zirconium halides is key to optimizing process conditions for the aforementioned applications, recent and accurate thermomechanical information for Zr halides remains scarce (3). In particular, for crystalline $ZrCl_4$ the low-temperature calorimetric measurements by Todd (7) and Efimov et al. (8), in the temperature ranges 52 − 296 K and 9 − 315 K, are still used as references (3). In addition, no comprehensive computational studies of the thermomechanical properties of $ZrCl_4$(cr) have been reported, to the best of our knowledge.

In this Letter, the lattice dynamics and thermomechanical properties of bulk monoclinic $ZrCl_4$(cr) have been studied within the framework of zero-damping dispersion-corrected density functional theory [DFT-D3(zero)]. Phonon calculations have been conducted within the quasi-harmonic approximation (QHA) and thermodynamic properties such as the entropy and isochoric and isobaric molar heat capacities have been derived and compared to available low-temperature calorimetric data. The thermal expansion and the evolution of the bulk modulus up to 550 K have also been predicted.

2. Computational methods

Total-energy calculations were carried out using Grimme's dispersion-corrected DFT (DFT-D3) (9), as implemented in the Vienna *ab initio* simulation package (VASP) (10). The exchange-correlation energy was computed using the generalized gradient approximation (GGA), with the parameterization of Perdew, Burke, and Ernzerhof (PBE) (11). Previous first-principles studies demonstrated that standard functionals, such as PBE, correctly reproduce the structure-properties relashionship of bulk zirconium and Zr alloys, as well as transition-metal chloride compounds (12, 13, 14, 15).

The projector augmented wave (PAW) method (16, 17) was utilized to model the interaction between valence electrons and ionic cores. In the Kohn-Sham (KS) equations, the Cl($3s^2, 3p^5$) and Zr($4p^6, 5s^2, 4d^2$) electrons were treated explicitly as valence electrons, and

*Corresponding author.
Email address: kimej@physics.unlv.edu (Eunja Kim)

PAW pseudopotentials were used to represent the remaining core electrons together with the nuclei. KS equations were solved using the blocked Davidson iterative matrix diagonalization scheme (18). A plane-wave cutoff energy of 500 eV was chosen for the electronic wavefunctions, ensuring total-energy convergence to within 1 meV/atom. Partial occupancies of the wavefunctions were controlled using Gaussian smearing, with a Gaussian width of 0.1 eV.

Simultaneous ionic and cell relaxations of $ZrCl_4$ were conducted, without symmetry constraints applied, using the quasi-Newton algorithm, and the Hellmann-Feynman forces acting on atoms were calculated with a convergence tolerance set to 0.01 eV/Å. The Brillouin zone (BZ) was sampled using the Monkhorst-Pack k-point scheme (19) with a k-point mesh of $5 \times 5 \times 5$

Initial structural optimization calculations with standard DFT/GGA/PBE for the bulk monoclinic $ZrCl_4$ unit cell (space group $P2/c$; IT No. 13; $Z = 2$) yielded lattice parameters of $a = 6.93$, $b = 8.16$ and $c = 6.35$ Å ($\alpha = \gamma = 90°$, $\beta = 107.6°$; $V = 342.0$ Å^3), considerably larger than X-ray diffraction (XRD) mesurements (20). This stems from the lack of a correct description of cohesive van der Waals interactions resulting from dynamical correlations between fluctuating charge distributions in standard DFT. Therefore, Grimme's dispersion-corrected DFT (DFT-D3) (9) was utilized in this study. This approach consists in adding a semi-empirical dispersion term, E_{disp}, to the Kohn-Sham GGA total-energy functional, *i.e.*, $E_{\text{DFT-D3}} = E_{\text{DFT-KS}} + E_{\text{disp}}$, where

$$E_{\text{disp}} = -\frac{1}{2}\sum_{i=1}^{N}\sum_{j=1}^{N}{\sum_{\mathbf{L}}}'\sum_{n=6,8}\left(f_{d,n}(r_{ij,L})\frac{C_{nij}}{r_{ij,L}^{n}}\right) \qquad (1)$$

where the summation runs over all N atoms and translations of the unit cell $\mathbf{L} = (\mathbf{l}_1, \mathbf{l}_2, \mathbf{l}_3)$, with the prime sign indicating that cell $i \neq j$ for $\mathbf{L} = \mathbf{0}$, C_{nij} and $r_{ij,L}$ are the averaged n^{th}-order dispersion coefficients and internuclear distance for the pair ij, and the damping functions in the zero damping DFT-D3 method [DFT-D3(zero)] are expressed as:

$$f_{d,n}(r_{ij}) = \frac{s_n}{1 + 6[r_{ij}/(s_{R,n}R_{0ij})]^{-\alpha_n}} \qquad (2)$$

with $R_{0ij} = (C_{8ij}/C_{6ij})^{1/2}$, $\alpha_6 = 14$, $\alpha_8 = 16$ and $s_{R,8} = 1$ are fixed parameters, and $s_6 = 0.5$, $s_8 = 0.722$ and $s_{R,6} = 1.217$ are PBE-optimized parameters (9).

In phonon calculations, the equilibrium structure $ZrCl_4$ was reoptimized with more stringent convergence, namely with thresholds set to 10^{-8} and 10^{-9} eV for electronic and ionic relaxations, respectively.

3. Results and discussion

The lattice parameters of bulk monoclinic $ZrCl_4$ calculated in the zero-temperature limit are $a = 6.38$, $b = 7.49$ and $c = 6.25$ Å ($\alpha = \gamma = 90°$, $\beta = 108.7°$; $V = 282.9$ Å^3; $c/a = 0.98$, $b/a = 1.17$), in excellent agreement with XRD values of $a = 6.361 \pm 0.004$, $b = 7.407 \pm 0.004$ and $c = 6.256 \pm 0.004$ Å ($\alpha = \gamma = 90 \pm 0.04°$, $\beta = 109.3 \pm 0.04°$; $V = 278.2$ Å^3; $c/a = 0.983$, $b/a = 1.164$) (20). The optimized $ZrCl_4$ unit-cell, featuring chains of edge-sharing coordination octahedra along the [001] direction, is depicted in Figure 1. The computed bond distances between Zr centers (2e Wyckoff positions) and apical and bridge Cl ligands (4g Wyckoff positions) are $d_{\text{Zr-Cl}_{\text{apical}}} = 2.33$ Å and $d_{\text{Zr-Cl}_{\text{bridge}}} = 2.50,\ 2.69$ Å. These bond distances compare well with the XRD values of $d_{\text{Zr-Cl}_{\text{apical}}} = 2.307$ Å and $d_{\text{Zr-Cl}_{\text{bridge}}} = 2.497,\ 2.656$ Å (20). The calculated (measured) Zr − Zr distance is 3.99 Å (3.962 Å), and the bond angles $\angle\text{Cl}_{\text{apical}}\text{ZrCl}_{\text{apical}}$ and $\angle\text{Cl}_{\text{bridge}}\text{ZrCl}_{\text{bridge}}$ are 100.9 and 79.6° (100.66 and 79.54°), respectively.

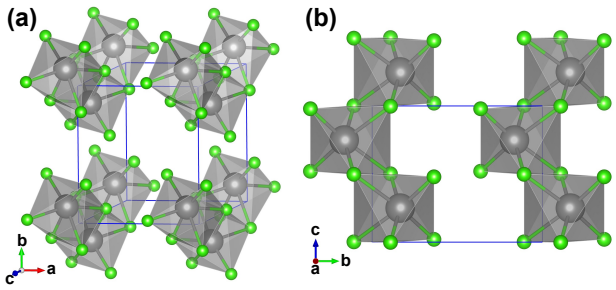

Figure 1: Crystal structure of bulk $ZrCl_4$ (space group $P2/c$; IT No. 13; $Z = 2$) optimized with DFT-D3(zero). (a) 3D-view of the unit cell; (b) top view in the (100) plane, with chains of edge-sharing coordination octahedra propagating along the [001] direction. The unit cell is represented by solid blue lines. Color legend: Cl, green; Zr, grey.

Phonon analysis was conducted using the finite-displacement method near equilibrium volume within the QHA in order to derive thermal properties of bulk $ZrCl_4$. A temperature effect was added to the calculated total energy $U(V)$ of the system through the phonon contribution, $F_{\text{phonon}}(T;V)$, expressed as:

$$F_{\text{phonon}}(T;V) = \frac{1}{2}\sum \hbar\omega + k_{\text{B}}T\sum \ln\left[1 - e^{-\beta\hbar\omega}\right], \qquad (3)$$

where $\hbar$ is Planck's reduced constant, $\hbar\omega$ is the energy of a single phonon with angular frequency ω, k_{B} is Boltzmann's constant, T is the temperature of the system, and $\beta = (k_{\text{B}}T)^{-1}$. The variation of $U(V) + F_{\text{phonon}}(T;V)$ as a function of the unit-cell volume in

the temperature range 0–550 K is displayed in Figure 2. Although the melting point of $ZrCl_4$ was reported as 710 ± 1 K, a monoclinic to cubic phase transformation around ≈ 538 K was discussed in previous studies (3). Therefore, the present calculations for monoclinic $ZrCl_4$(cr) are limited to temperatures below ≈ 550 K. Results show an overall unit-cell volume increase with temperature.

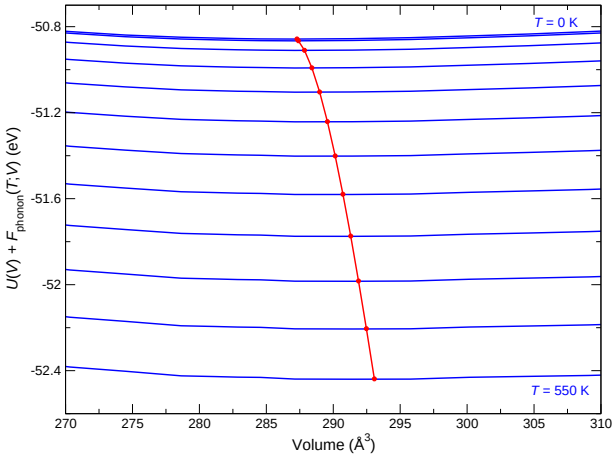

Figure 2: Variation of the total energy with phonon contribution, $U(V) + F_{\text{phonon}}(T; V)$, of bulk $ZrCl_4$ as a function of the unit-cell volume calculated with DFT-D3(zero) from T = 0 to 550 K, by steps of 50 K. The local minimum of each free energy curve is indicated by a sold red circle.

At constant hydrostatic pressure P, the Gibbs free energy, G, was obtained by the following transformation to introduce a volume dependence (21):

$$G(T, P) = \min_{\text{V}} \Big[U(V) + F_{\text{phonon}}(T; V) + PV \Big], \quad (4)$$

where $\min_{\text{V}}$[function of V] corresponds to a unique minimum of the expression between brackets with respect to the unit-cell volume V. $U(V) + F_{\text{phonon}}(T; V)$ was computed as discussed above, and the thermodynamic functions of Eq. (4) were fitted to the universal Vinet equation of state (22), *i.e.*,

$$P(V) = 3K_0 \frac{(1-x)}{x^2} \exp\left[\frac{3}{2}(K_0' - 1)(1-x)\right], \quad (5)$$

with $x = (V/V_0)^{1/3}$, where V_0 and V are the equilibrium and deformed unit-cell volumes, respectively, and the bulk modulus, K_0, and its derivative with respect to the pressure, K_0', are calculated according to:

$$K_0(T) = -V\left(\frac{\partial P}{\partial V}\right)_{P=0} \text{ and } K_0'(T) = \left(\frac{\partial K}{\partial P}\right)_{P=0}. \quad (6)$$

The computed thermal evolutions of K_0 and K_0' are shown in Figure 3. The bulk modulus and its pressure derivative are predicted to vary from K_0 = 8.7 to 7.0 GPa and from K_0' = 10.4 to 8.9 GPa between 0 and 550 K. Interestingly, both K_0 and K_0' do not decrease monotonically with temperature, but exhibit instead maxima in the vicinity of ≈ 20 and 80 K, respectively.

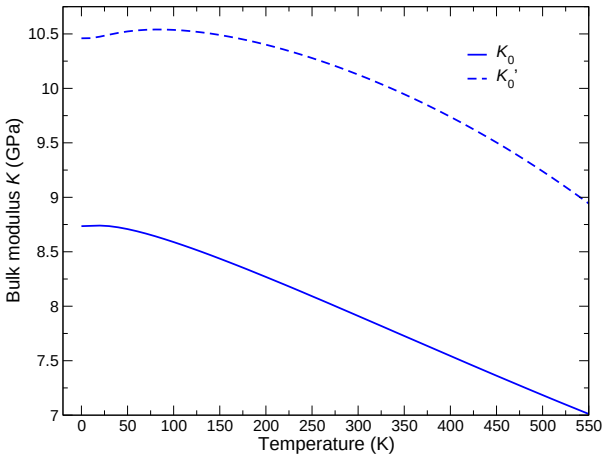

Figure 3: Thermal evolution of the bulk modulus (K_0) and its pressure-derivative (K_0') for $ZrCl_4$ calculated using the Vinet equation of state with DFT-D3(zero).

In order to investigate the origin of this anomaly, the thermal expansion, $\alpha = V^{-1}(\partial V/\partial T)_P$ was calculated, along with the Grüneisen parameter, $\gamma = -d(\ln \nu)/d(\ln V)$, where ν is the vibrational mode frequency. Vibrational modes whose frequency decreases with a contraction of the unit-cell volume V are characterized by $\gamma < 0$, and tend to produce negative contributions to the overall thermal expansion (23). This stems from the Grüneisen relationship connecting α and γ, i.e., $\alpha = \gamma C_{\text{V}} K/V$, where K is the bulk modulus and the isochoric molar heat capacity C_{V} is defined as,

$$C_{\text{V}} = k_{\text{B}} \sum (\beta\hbar\omega)^2 \frac{e^{\beta\hbar\omega}}{[e^{\beta\hbar\omega} - 1]^2}, \quad (7)$$

As shown in Figure 4, bulk monoclinic $ZrCl_4$ undergoes negative thermal expansion (NTE; $\alpha < 0$) below $T \approx$ 17 K, with minimum values of the thermal expansion of $\alpha = -1.2 \times 10^{-6}$ K^{-1} and the Grüneisen parameter of $\gamma = -1.1$ reached near $T \approx 10$ K. Such NTE behavior is typical of low-energy transverse vibrational modes with $\gamma < 0$, which are populated at low temperature (23).

The isobaric molar heat capacity, C_{P}, was also derived as the second derivative of the Gibbs free energy

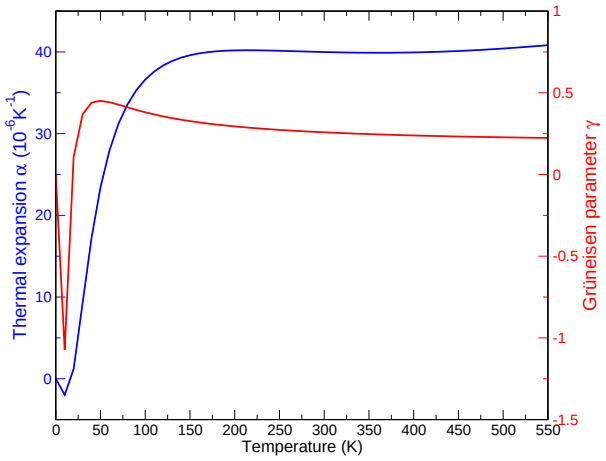

Figure 4: Thermal expansion (α) and Grüneisen paramter (γ) of bulk $ZrCl_4$ calculated with DFT-D3(zero).

[see Eq. (4)] with respect to the temperature:

$$\begin{aligned} C_{\rm P}(T,P) &= -T\frac{\partial^2 G(T,P)}{\partial T^2} \\ &= T\frac{\partial V(T,P)}{\partial T}\frac{\partial S(T,V)}{\partial V}\Big|_{V=V(T,P)} \\ &\quad + C_{\rm V}[T,V(T,P)], \end{aligned} \tag{8}$$

with $C_{\rm V}$ defined in Eq. (7) and where $V(T,P)$ denotes the equilibrium volume at T and P, and the entropy is computed using the formula:

$$S = -k_{\rm B}\sum \ln\left[1-e^{-\beta\hbar\omega}\right] - \frac{1}{T}\sum\frac{\hbar\omega}{e^{\beta\hbar\omega}-1}. \tag{9}$$

Figure 5 displays the computed entropy, isochoric molar heat capacity, and isobaric molar heat capacity at standard pressure (P = 1 bar) for bulk $ZrCl_4$, along with the low-temperature heat capacity measurements by Todd (7) and Efimov et al. (8) in the temperature ranges $T = 52-296$ K and $9-315$ K, respectively. The standard values calculated at T = 298.15 K in this study are $C_{\rm P}^0$ = 107.3 J mol^{-1} K^{-1} and $S_{\rm P}^0$ = 162.1 J mol^{-1} K^{-1}, significantly smaller than the data of $C_{\rm P}^0$ = 119.87 J mol^{-1} K^{-1} and $S_{\rm P}^0 = 186.19\pm2.1$ J mol^{-1} K^{-1} collected by Todd at 298.16 K (7) and the calorimetric values of $C_{\rm P}^0 = 116.80\pm0.20$ J mol^{-1} K^{-1} and $S_{\rm P}^0 = 180.40\pm0.35$ J mol^{-1} K^{-1} reported by Efimov et al. (8) at 298.15 K. However, the stoichiometric $ZrCl_4$(cr) characterized by Todd contained hafnium impurities, and a correction increasing the measured $C_{\rm P}$ was applied [see ref. (7) for details]. In addition, while the $ZrCl_4$(cr) sample investigated by Efimov et al. was free from Hf, Ti, Ta, Nb (mass fractions $< 10^{-6}$), it contained Cu, Fe and Si impurities (mass fractions of $\approx 10^{-5}$), which might also affect heat capacity measurements (8).

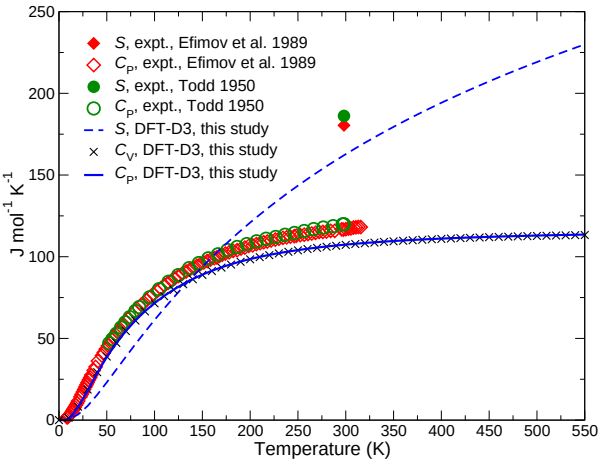

Figure 5: Entropy (S), isochoric molar heat capacity ($C_{\rm V}$), and isobaric molar heat capacity at standard pressure ($C_{\rm P}$) of $ZrCl_4$ calculated with DFT-D3(zero). Calorimetric data from Todd [Ref. (7)] and Efimov et al. [Ref. (8)] are also represented.

4. Conclusions

In summary, DFT-D3(zero) calculations were conducted to investigate the the lattice dynamics and themomechanical properties of bulk monoclinic $ZrCl_4$(cr). Phonon calculations predict that low-temperature negative thermal expansion occurs in $ZrCl_4$(cr) below $\approx$ 17 K, with Da a coefficient of thermal expansion of $\alpha = -1.2$ ppm K^{-1} and a Grüneisen parameter of $\gamma = -1.1$. Such NTE has limited impact on the thermal variation of the bulk modulus and its pressure-derivative, the former varying from K_0 = 8.7 to 7.0 GPa in the range 0–550 K. The computed isobaric molar heat capacity derived from phonon calculations within the quasi-harmonic approximation underestimates existing calorimetric data by up to $8-10\%$ at room temperature. Such discrepancies might stem in part from the presence of impurities (e.g., Hf, Cu, Fe or Si) in the samples characterized. Therefore, new heat-capacity measurements for high-purity $ZrCl_4$(cr) are desirable, especially above room temperature where calorimetric data are scarce.

Acknowledgments

This research was performed using funding received from the U.S. Department of Energy, Office of Nuclear

Energy's Nuclear Energy University Program (NEUP). Sandia National Laboratories is a multi-mission laboratory managed and operated by National Technology and Engineering Solutions of Sandia, LLC., a wholly owned subsidiary of Honeywell International, Inc., for the U.S. Department of Energy's National Nuclear Security Administration under contract DE-NA0003525.

References

[1] G. Homerin, D. Baudelet, P. Dufrénoy, B. Rigo, E. Lipka, X. Dezitter, C. Furman, R. Millet, A. Ghinet, Tetrahedron Letters 57 (2016) 1165.
[2] B. Lustman, J. F. Kerze, *The metallurgy of zirconium*, Mc Graw Hill: New York, NY, 1955.
[3] M. G. M. van der Vis, E. H. P. Cordfunke, R. J. M. Konings, Thermochimica Acta 302 (1997) 93.
[4] A. E. Bohé, J. J. Andrade Gamboa, D. M. Pasquevich, Mater. Sci. Technol. 13 (1997), 865.
[5] E. D. Collins, G. D. DelCul, B. B. Spencer, R. R. Brunson, J. A. Johnson, D. S. Terekhov, N. V. Emmanuel, Procedia Chemistry 7 (2012) 72.
[6] T. Ogawa, K. Fukuda, S. Kashimura, T. Tobita, F. Kobayashi, S. Kado, H. Miyanishi, I. Takahashi, T. Kikuchi, J. Am. Ceram. Soc. 75 (1992), 2985.
[7] S. S. Todd, J. Am. Chem. Soc. 72 (1950) 2914.
[8] M. E. Efimov, I. V. Prokopenko, V. A. Medvedev, G. A. Berezovskii, I. E. Paukov, J. Chem. Thermodynamics 21 (1989) 677.
[9] S. Grimme, J. Antony, S. Ehrlich, S. Krieg, J. Chem. Phys. 132 (2010) 154104.
[10] G. Kresse, J. Furthmüller, Phys. Rev. B 54 (1996) 11169.
[11] J. P. Perdew, K. Burke, M. Ernzerhof, Phys. Rev. Lett. 77 (1996) 3865.
[12] P. F. Weck, E. Kim, F. Poineau, E. E. Rodriguez, A. P. Sattelberger, K. R. Czerwinski, Inorg. Chem. 48 (2009), 6555.
[13] F. Poineau, C. D. Malliakas, P. F. Weck, B. L. Scott., E. V. Johnstone, P. M. Forster, E. Kim, M. G. Kanatzidis, K. R. Czerwinski, A. P. Sattelberger, J. Am. Chem. Soc. 133 (2011) 8814.
[14] C. D. Malliakas, F. Poineau, E. V. Johnstone, P. F. Weck, E. Kim, B. L. Scott, P. M. Forster, M. G. Kanatzidis, K. R. Czerwinski, A. P. Sattelberger, J. Am. Chem. Soc. 135 (2013) 15955.
[15] P. F. Weck, E. Kim, V. Tikare, J. A. Mitchell, Dalton Trans. 44 (2015) 18769.
[16] P. E. Blöchl, Phys. Rev. B 50 (1994) 17953.
[17] G. Kresse, D. Joubert, Phys. Rev. B 59 (1999) 1758.
[18] E. R. Davidson, in *Methods in Computational Molecular Physics*, G. Diercksen, and S. Wilson; Eds.; NATO Advanced Study Institute, Series C, Plenum: New York, NY, 1983, vol. 113, p. 95.
[19] H. Monkhorst, J. Pack, Phys. Rev. B 13 (1976) 5188.
[20] B. Krebs, Angew. Chem. 81 (1969) 120.
[21] A. Togo, F. Oba, I. Tanaka, Phys. Rev. B 78 (2008) 134106.
[22] P. Vinet, J. R. Rose, J. Ferrante, J. R. Smith, J. Phys.: Condens. Matter, 1 (1989) 1941.
[23] J. S. O. Evans, J. Chem. Soc., Dalton Trans. (1999) 3317.

Graphical abstract

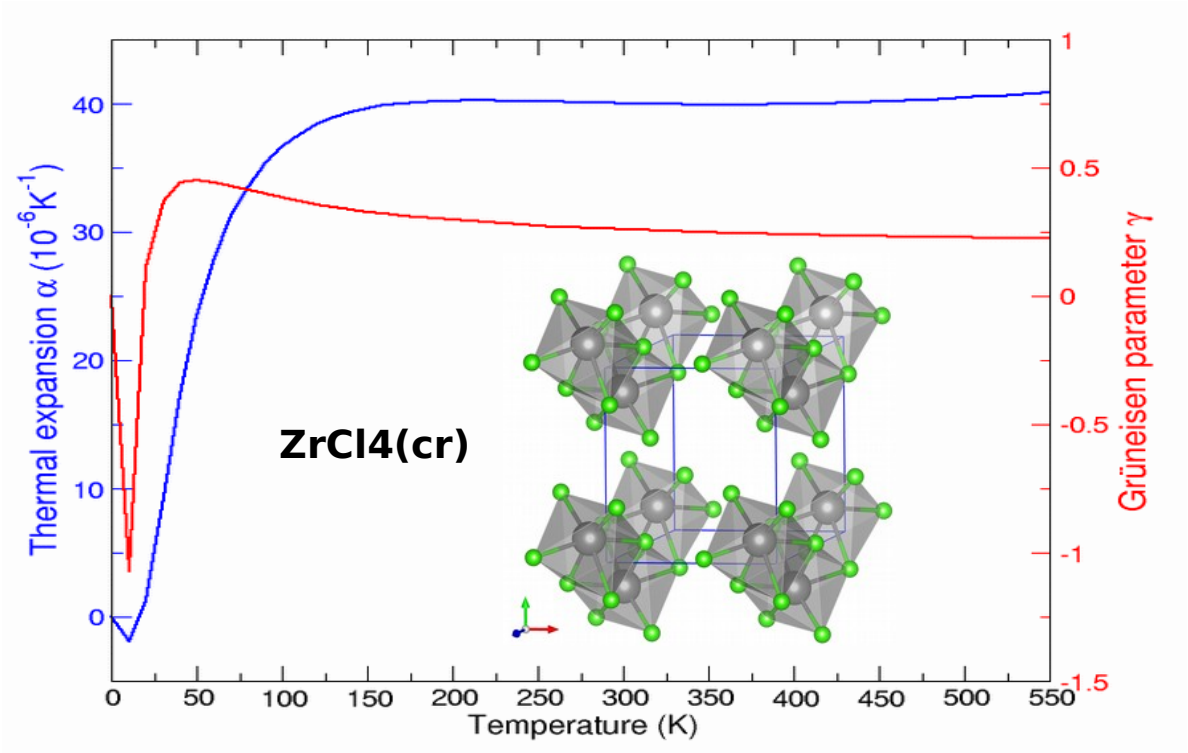

Highlights

• The lattice dynamics of ($ZrCl_4$) was investigated with DFT-D3(zero). • $ZrCl_4$(cr) exhibits negative thermal expansion below $T \approx 17$ K. • The computed thermal expansion and Grüneisen parameter are $\alpha = -1.2$ ppm K^{-1} and $\gamma = -1.1$ near 10 K. • The computed isobaric molar heat capacity underestimates calorimetric data by up to 10% at 298 K.